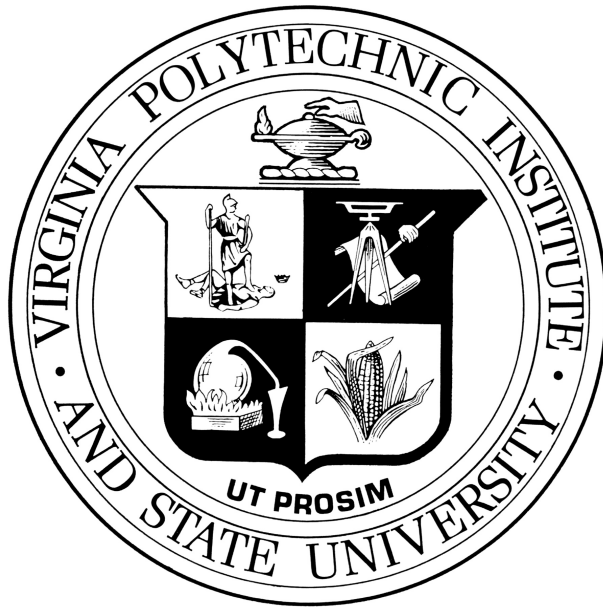


VIRGINIA POLYTECHNIC INSTITUTE AND STATE UNIVERSITY

BRADLEY DEPARTMENT OF ELECTRICAL AND COMPUTER
ENGINEERING



MIMO Final Project

Author

Gaurav Duggal

Instructor

Dr. Michael Buehrer

December 13, 2022

Contents

1	Introduction	1
2	Description	1
2.1	Input	1
3	Validation	1
3.1	Q1. MIMO time-varying and frequency selective channel	1
3.1.1	Introduction	1
3.1.2	Channel Mathematical Model	2
3.1.3	Plots	3
3.2	Q2. Q3. Spatial MIMO OFDM	5
3.2.1	Introduction	5
3.2.2	Q2a). Space-time coding for MIMO-OFDM	5
3.2.3	Q2b). Spatial Multiplexing	7
3.2.4	Q2c). MIMO OFDM channel estimation for spatial multiplexing	9
3.2.5	Q3a). Bit-loading for spatial multiplexing for MIMO-OFDM	11
3.3	Q4a).: Time and frequency synchronization	14
3.3.1	Introduction	14
3.3.2	System model and Results	15
4	Conclusion	18

1 Introduction

In this assignment, We implement a time-varying and frequency-selective channel and then implement various MIMO OFDM techniques to increase throughput and also to estimate the channel.

2 Description

2.1 Input

The inputs are summarised below

- N : number of sub-carriers
- τ_{rms} Delay spread
- fd_{max} Doppler spread
- AoA, AoD Angular spread
- N_{trials} : Number of trials of the experiment
- fs : Sampling frequency
- k : number of bits/symbol
- M_r Receive Antennas
- N_t transmit Antennas

3 Validation

3.1 Q1. MIMO time-varying and frequency selective channel

3.1.1 Introduction

For a $M_r \times N_t$ MIMO system, we have $M_r N_t$ possible channels. Here M_r is the number of the receive antennas and N_t is the number of transmit antennas. Due to multi-path reception, each of these channels is frequency selective. Additionally, due to the Doppler spread due to relative transmitter-receiver motion, the channel is time-varying and the Doppler spreads decides the channel coherence time. Some of the multi-path can be resolved as it is a function of the signal bandwidth. Empirically it has been shown that the resolvable multi-path reception follows

an exponential power delay profile. Also, we assume that the delay spread that characterizes the multi-path is much smaller than the duration of the symbol. The inverse of the signal bandwidth B Hz is the resolution of the multi-path reception and is represented by L channel taps.

3.1.2 Channel Mathematical Model

The k^{th} channel tap for $M_r \times N_t$ MIMO channel at time t is given by

$$\mathbf{H}^k(t) = \sqrt{\frac{\sigma_k^2}{N}} \sum_{i=1}^N \underbrace{e^{j(2\pi f_{dmax} \phi_{i,k} t + \phi_{i,k})}}_{\text{Doppler}} \underbrace{e^{j(-2\frac{\pi}{\lambda} \mathbf{d} \sin \theta_{i,k})}}_{\text{AoA}(M_r \times 1)} \underbrace{e^{j(-2\frac{\pi}{\lambda} \mathbf{\Delta} \sin \phi_{i,k})}}_{\text{AoD}(1 \times N_t)} \quad (1)$$

where the i^{th} non-resolvable path has Doppler, receive AoA and transmit AoD modeled by the first, second, and third terms inside the summation in the equation. The amplitude of the k^{th} tap is found by the Power Delay Profile (PDP) exponential distribution. The AoA and AoD angle distribution is assumed to be zero mean Gaussian or uniform distribution.

Important Assumptions:

1. We assume that the time axis represented by variable t is sampled with a sampling time $TS = N \cdot ts$ where, ts is the fast time sampling time and N is the number of sub-carriers. This assumes that the time-varying channel is constant for at least one OFDM symbol duration and hence assumes there can be **no Inter-Carrier-Interference (ICI)**. For the purpose of this assignment, since the Doppler spread is low, this is a reasonable assumption. Also this means we can use the regular convolution operator that assumes LTI nature thereby avoiding implementing the time-varying convolution.
2. We have L channel taps which represent the contain the L resolvable significant power paths and are sampled along the fast time ts .

3.1.3 Plots

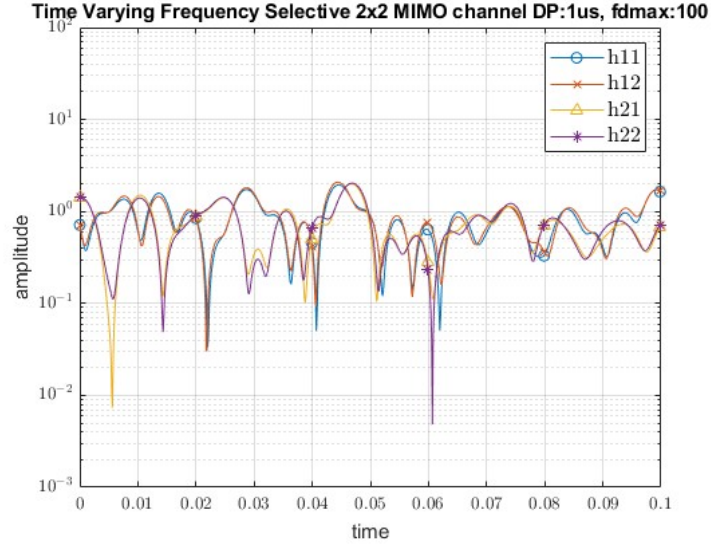


Figure 1: Time-varying nature of the 2×2 MIMO channel demonstrated for delay spread = $1\mu s$, Doppler spread 100Hz

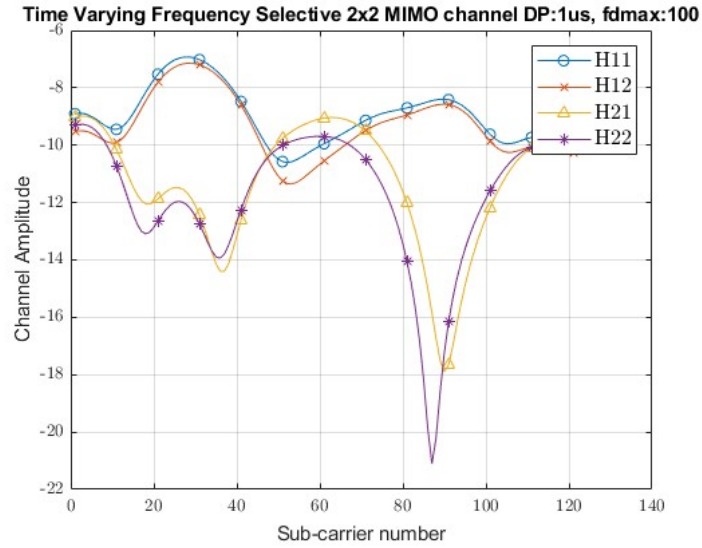


Figure 2: Frequency selective nature of the 2×2 MIMO channel demonstrated for delay spread = $1\mu s$, Doppler spread 100Hz

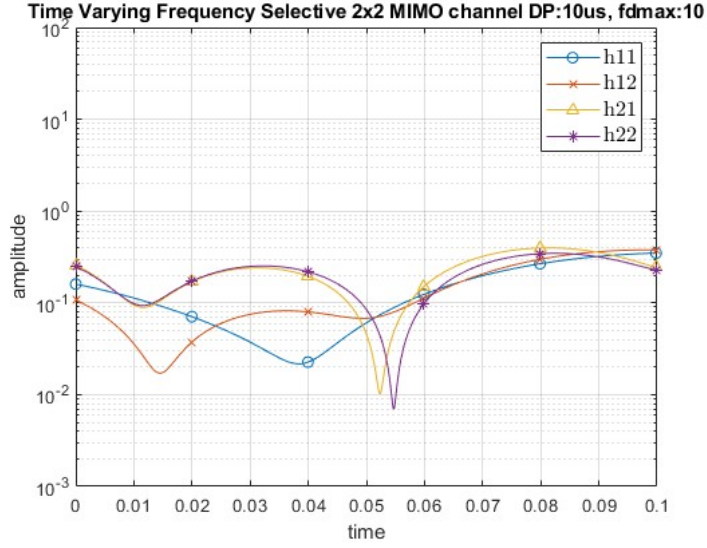


Figure 3: Time-varying nature of the 2×2 MIMO channel demonstrated for delay spread = $10\mu s$, Doppler spread 10Hz

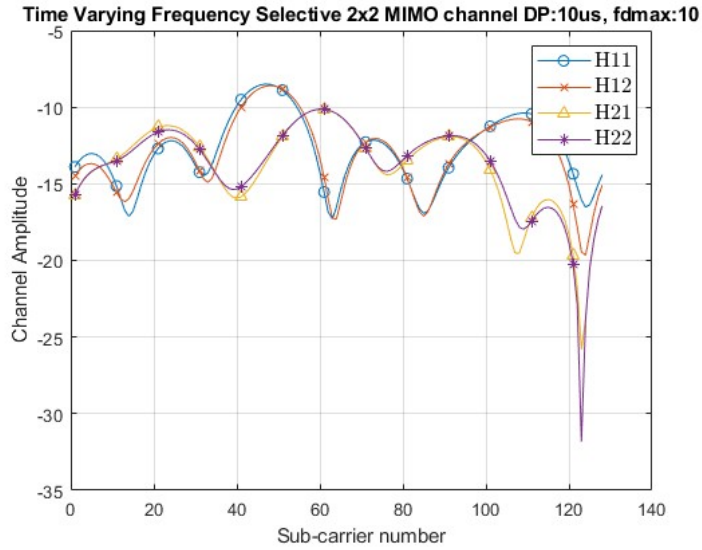


Figure 4: Frequency selective nature of the 2×2 MIMO channel demonstrated for delay spread = $10\mu s$, Doppler spread 10Hz

The channel spatial correlation does not change with Doppler spread or delay spread. For angle spread 5° at the tx and angle spread 360° at the receiver the channel correlation is:

Table 1: Channel correlation of THE 1st tap across time

CH.	h11	h12	h21	h22
h11	1	0.98	0.40	0.35
h12	0.98	1	0.42	0.39
h21	0.40	0.42	1	0.97
h22	0.35	0.39	0.97	1

3.2 Q2. Q3. Spatial MIMO OFDM

3.2.1 Introduction

In real systems, we aim to achieve as high a throughput as possible. Throughput is the product of two terms i.e. $(1 - \text{PER})$ and packet size. Here, PER is the packet error rate. Therefore our goal is to reduce the packet errors for a given packet size or increase the packet size keeping the packet error rate the same. To exploit spatial diversity we can use Space-time block codes (STBC). This will result in lower packet error rates. Following this, we use spatial multiplexing using multiple antennas to increase the throughput. Later in this section, we also explore the tradeoff between increasing the number of pilots to achieve better channel estimates at the cost of reducing the packet size hence impacting the overall throughput.

3.2.2 Q2a). Space-time coding for MIMO-OFDM

In this section, we explore the application of the Alamouti codes to exploit spatial diversity for a 2×2 MIMO OFDM system. For each TX antenna we transmit two OFDM symbols according to below:

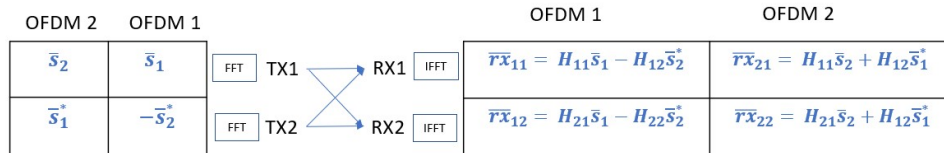


Figure 5: Alamouti 2×2 MIMO OFDM system model

Note that $\bar{H}_{ij}i, j \in (1, 2)$ are $N \times N$ diagonal matrices with the diagonal containing the frequency domain channel. Both \bar{s}_1 and \bar{s}_2 are OFDM symbols with N sub-carriers each carrying data symbols. In this system, we consider that our packet contains four OFDM symbols spanning two tx antennas and two OFDM symbol durations. At the receiver, we get four measurements over two time slots and two receive antennas. Assuming perfect channel knowledge, we can estimate the transmitted

symbols using the equations below:

$$\hat{s}_1 = \frac{H_{11}^* \bar{r}_{11} + H_{12} \bar{r}_{21}^*}{|H_{11}|^2 + |H_{12}|^2}$$

$$\hat{s}_2 = \frac{-H_{22} \bar{r}_{12}^* + H_{21}^* \bar{r}_{22}}{|H_{22}|^2 + |H_{21}|^2}$$
(2)

For $N = 128$ subcarriers on each OFDM symbol and QPSK modulation and approximately a half-rate BCH code, we get a total of 250 data bits per packet. The error correction code is able to correct up to 31 errors in a packet. The throughput is calculated for all packets with zero errors received after error correction. We compare this to a theoretical 1×1 OFDM system with QPSK modulation.

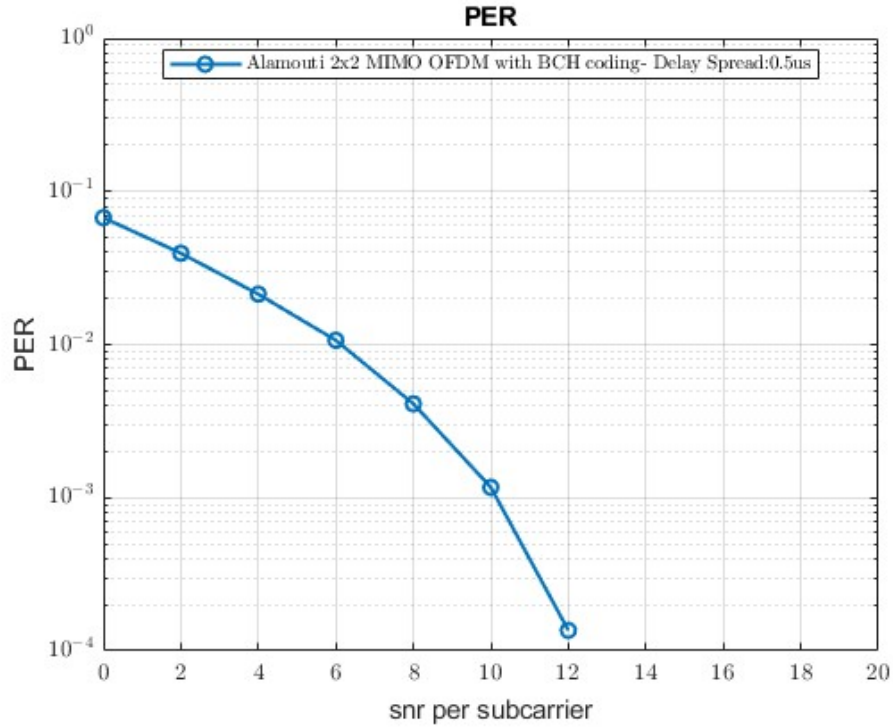


Figure 6: Alamouti 2×2 MIMO OFDM Packet Error Rate with BCH coding

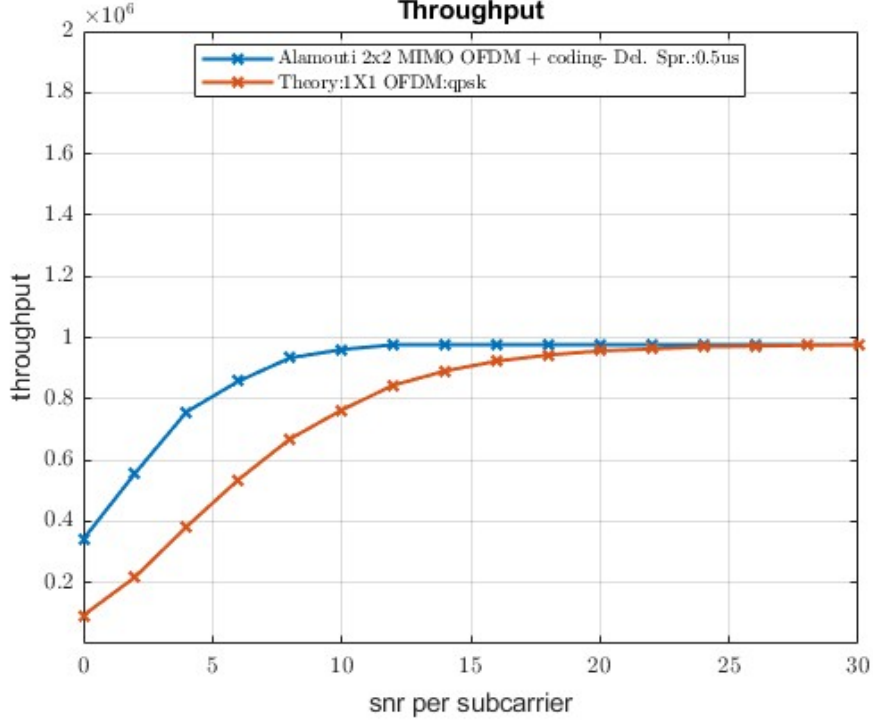


Figure 7: Alamouti 2×2 MIMO OFDM Throughput with BCH coding

Since we transmit 250 data bits over two time slots over two transmit antennas in the STBC system, we expect to have the same throughput as a theoretical 1×1 QPSK modulated OFDM system. This is because the latter only uses one time-slot to transmit the 250 data bits. However, the two transmitters offer spatial diversity hence for lower SNR's we see better performance from the STBC-based system in terms of throughput whereas at high SNR it converges to the theoretical system.

3.2.3 Q2b). Spatial Multiplexing

We use spatial modulation to increase throughput. There are multiple spatial multiplexing techniques and among all the techniques we explore spatial multiplexing without feedback to the transmitter. The system model is as below:

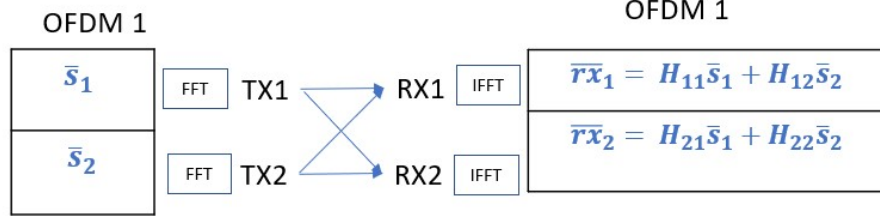


Figure 8: Spatial 2×2 MIMO OFDM system model

In Fig.8, $H_{ij}, i, j \in (1, 2)$ are $N \times N$ matrices with the frequency domain channel along the main diagonal. At the receiver, in the interest of good performance with relatively less complexity we use a linear receiver architecture. The system model in Fig.8 can be written as

$$\bar{r} = H\bar{s} + \bar{n}$$

$$H = \begin{bmatrix} H_{11} & H_{12} \\ H_{21} & H_{22} \end{bmatrix} \quad \bar{s} = \begin{bmatrix} s_1 \\ s_2 \end{bmatrix} \quad \bar{r} = \begin{bmatrix} \bar{r}_1 \\ \bar{r}_2 \end{bmatrix} \quad (3)$$

The MMSE processing is given by

$$T_{mmse} = \sqrt{\frac{N_t}{E_s}} \left(\mathbf{H}^H \mathbf{H} + \frac{N_t N_o}{E_s} \mathbf{I} \right)^{-1} \mathbf{H}^H \quad (4)$$

The decision variables are given by

$$z = T_{mmse} \bar{r}. \quad (5)$$

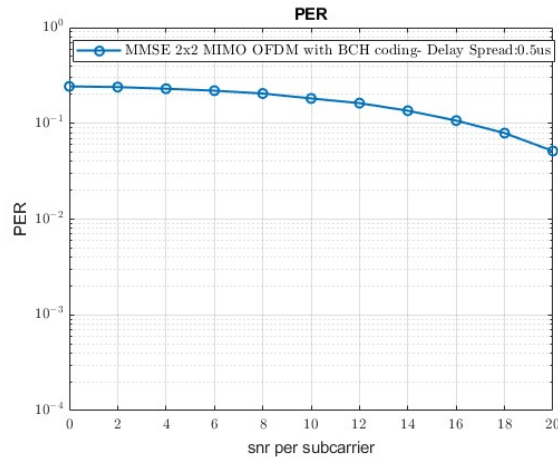


Figure 9: Spatial multiplexing 2×2 MIMO OFDM Packet Error Rate with half rate BCH coding with MMSE receiver

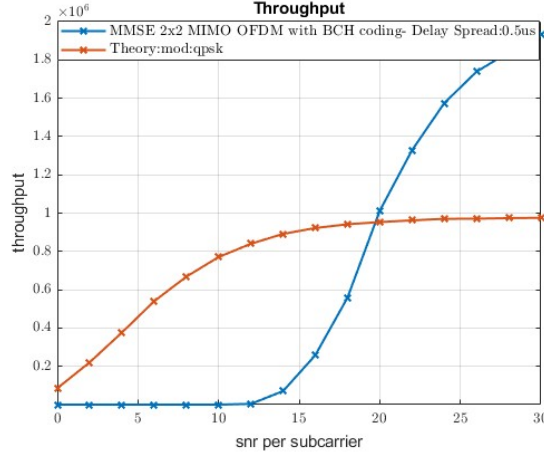


Figure 10: Spatial multiplexing 2×2 MIMO OFDM Throughput with half rate BCH coding with MMSE receiver

We observe that spatial multiplexing has a lower packet error rate compared to the Alamouti 2×2 scheme however, at high SNRs offers much higher throughput. This demonstrates the multiplexing-diversity tradeoff in MIMO communications. Note ideally we should be comparing the MLE decoder however due to its exponential complexity it is computationally very costly to implement. Key assumptions for this simulation:

1. A packet consists of two OFDM symbols across the two TX antennas.
2. BCH code with 511 encoded bits with 250 data bits was used. This offered 31 bits of error correction capability.
3. The throughput is calculated using $(1 - PER) \times D_p$ where D_p is the number of data bits in a packet which is 250 in our case.

3.2.4 Q2c). MIMO OFDM channel estimation for spatial multiplexing

We have done channel estimation for OFDM for a single antenna system in previous assignments so the detector design will remain the same as before. The key idea here is that in our 2×2 MIMO system, we have four channels that need to be estimated. Each antenna sends one OFDM symbol containing pilots and at each receiver, we get the resultant sum of the two OFDM symbols transmitted. After performing the receive side FFT processing and converting the received signal into the frequency domain, we can separate the information-carrying symbols across sub-carriers. For channel estimation we need to ensure the pilots from each transmitting antenna can be separated at each receiver. We place pilots on sub-carrier indices p_1 on transmit Antenna 1 and, on indices p_2 for transmit Antenna 2. Now in order to make the pilots on the different antennas orthogonal at

each receiver we null sub-carrier indices p_2 and p_1 on Antenna 1 and Antenna 2 respectively. This is visualized in the system design below:

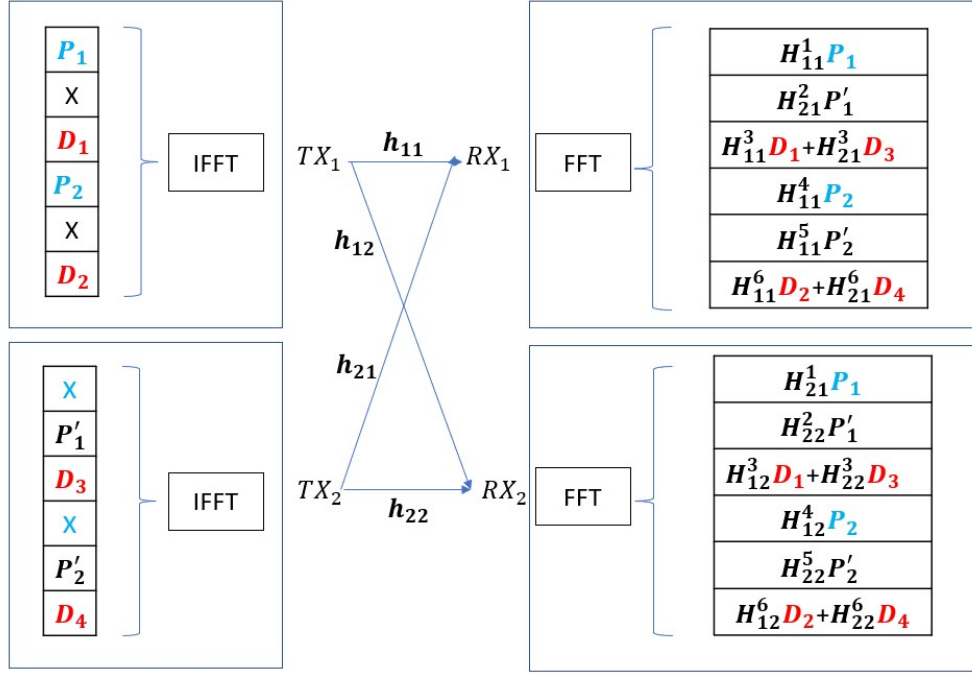


Figure 11: Channel estimation for spatial multiplexing in MIMO OFDM

Note: for a 2×2 MIMO -OFDM system we could use the Alamouti scheme to orthogonalize the pilots at the receiver without needing to NULL any pilot locations thereby increasing the received power for each pilot measurement at the receiver, however in the simulation the system design in Fig. 11 is implemented.

$$\begin{aligned}
 \mathbf{Q}^\dagger &= \left(\mathbf{Q}_{N_p L}^H \mathbf{Q}_{N_p L} \right)^{-1} \mathbf{Q}_{N_p L}^H \\
 \hat{\mathbf{h}}_{11}^{(LS)} &= \mathbf{Q}^\dagger \mathbf{P}_1^{-1} \mathbf{e}_{p_1}^{rx_1} \\
 \hat{\mathbf{h}}_{12}^{(LS)} &= \mathbf{Q}^\dagger \mathbf{P}_2^{-1} \mathbf{e}_{p_2}^{rx_1} \\
 \hat{\mathbf{h}}_{21}^{(LS)} &= \mathbf{Q}^\dagger \mathbf{P}_1^{-1} \mathbf{e}_{p_1}^{rx_2} \\
 \hat{\mathbf{h}}_{22}^{(LS)} &= \mathbf{Q}^\dagger \mathbf{P}_2^{-1} \mathbf{e}_{p_2}^{rx_2}.
 \end{aligned} \tag{6}$$

Here, $\mathbf{e}_{p_j}^{rx_i}$ is the error vector on the i^{th} rx antenna antenna at sub-carrier indices p_j , \mathbf{P}_j are the pilots for the j^{th} tx antenna. The data can be decoded on the data sub-carriers using (5). In this simulation we have not used an error correction code, instead assumed there is a half-rate error correction code and the packet error and throughput are calculated based on the transmitted bits.

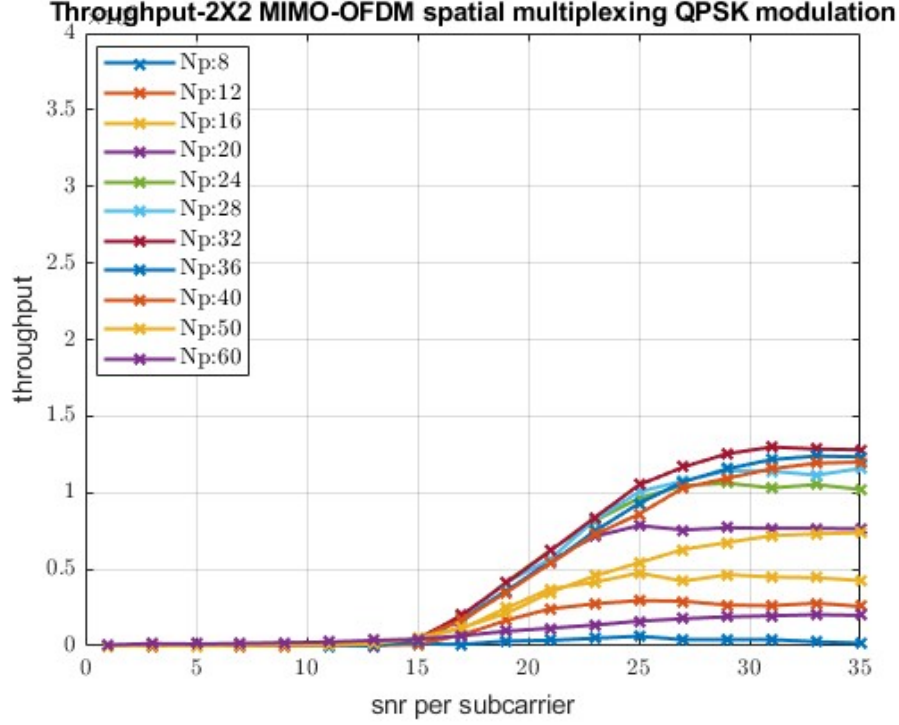


Figure 12: Throughput vs Number of pilots for spatial multiplexing in a 2×2 MIMO OFDM system. The receiver structure is MMSE.

There is a fundamental tradeoff between the number of pilots and throughput. If we increase pilots we can drive the packet error rate lower however that also reduces the packet size since we are left with fewer sub-carriers to carry data. If the number of pilots is too low, then even though our packet size is larger, the packet error ends up reducing the throughput. From Fig.11 the optimal number of pilots to maximize the throughput is found to be 32.

3.2.5 Q3a). Bit-loading for spatial multiplexing for MIMO-OFDM

Until now we have exploited the spatial characteristics of the channel using space-time modulation or spatial multiplexing techniques. We have also seen how OFDM can exploit frequency diversity in a frequency-selective channel. In this section, we combine the two together and hence we can increase the throughput. In the current channel model we have a low angular spread at the transmitter hence we have two pairs of correlated channels. Using the two independent channels i.e. h_{11} and h_{12} (or h_{21} and h_{22}) can be used to get the optimal modulation schemes per sub-carrier. The only difference is to run the algorithm over only the data-carrying sub-carriers.

Algorithm for maximizing Throughput:

1. Set the maximum modulation scheme on all N sub-carriers.

2. Calculate the SNR on all the sub-carriers
3. Calculate the BER b_n based on the modulation scheme and SNR on the sub-carrier. Note b_n is obtained by using the theoretical BER expressions for M-QAM in an AWGN channel with known SNR and order M.
4. Calculate the Average BER.
5. while the Average BER is above the target BER, keep looping
6. Select the sub-carrier index with the highest BER and reduce the modulation order. If the modulation order is BPSK, disable the sub-carrier i.e. transmit 0 on that sub-carrier.
7. Calculate the Avg BER using and exit if below target BER else go back to step 5.

The throughput is calculated by the product of (1-packet error rate) and the packet size divided by the packet duration.

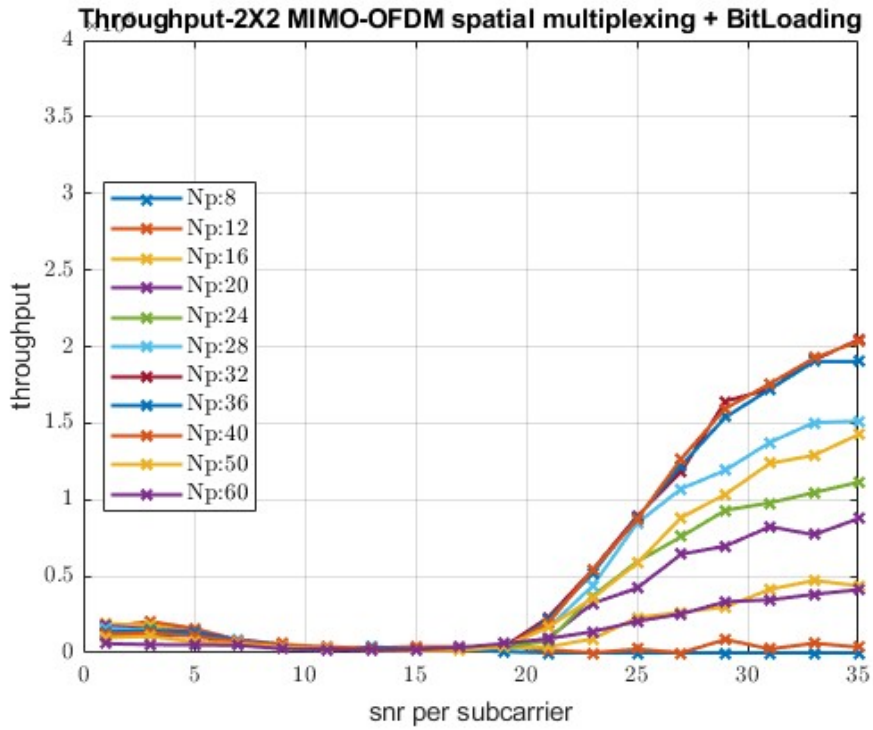


Figure 13: Throughput vs Number of pilots for spatial multiplexing in a 2×2 MIMO OFDM system. The receiver structure is MMSE.

We observe that by using Bit-Loading and spatial multiplexing by using MIMO OFDM, we can exploit both frequency diversity as well as spatial diversity. Comparing Fig.12 with Fig.13

we observe that the former shows lower throughput compared to the latter as in the latter we have additionally exploited frequency diversity using Bit-Loading.

There are several ways to improve this system:

1. We could use transmitter feedback-based spatial multiplexing techniques like Eigen-beamforming since the transmitters are correlated and it might show better performance gains.
2. We could use better-performing receiver structures like SIC+MMSE to get better performance at the cost of extra computations.
3. We could increase the SNR for the pilots at the receiver without increasing the number of pilots by using Alamouti coding. This will make the pilots from the two transmitters orthogonal at the receivers without needing to null any sub-carriers.

I expected better performance using bit-loading, so I increased the Angular spread at the transmitter and made the channel more frequency selective. Below are the Throughput plots with QPSK and Bit-loading and we can see a very big increase in throughput. Also, we note that the number of pilots required to get good throughput has increased to approx 36-40 compared to 28-32 earlier.

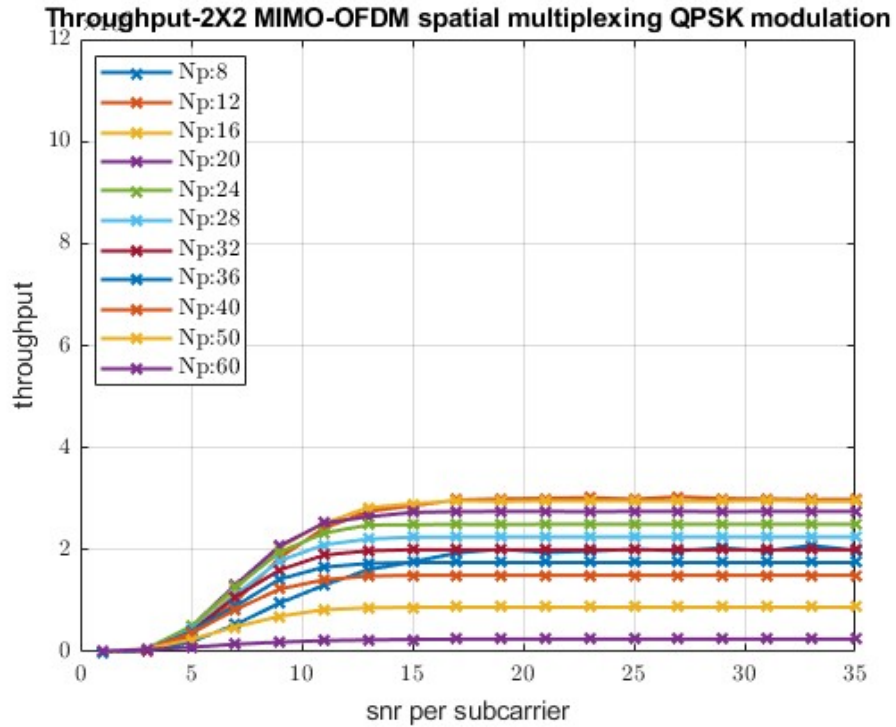


Figure 14: Throughput vs Number of pilots for spatial multiplexing in a 2×2 MIMO OFDM system in a spatially uncorrelated and highly frequency selective channel. The receiver structure is MMSE.

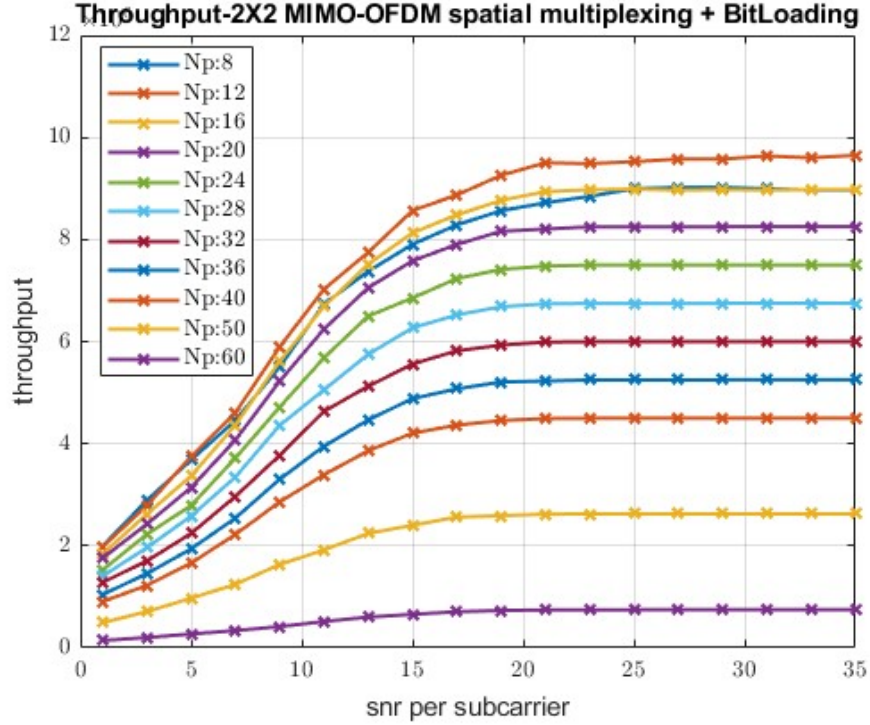


Figure 15: Throughput vs Number of pilots for spatial multiplexing in a 2×2 MIMO OFDM system in a spatially uncorrelated and highly frequency selective channel. The receiver structure is MMSE.

3.3 Q4a).: Time and frequency synchronization

3.3.1 Introduction

When the transmitter transmits, the receiver gets the signal after a certain delay depending on the signal propagation distance. The receiver is switched on at an arbitrary time not synchronized with the transmitter and starts receiving symbols starting at an arbitrary time. The receiver needs to find the start of the OFDM symbols, and the frame start and end time to do the rest of the signal processing. This is known as time synchronization.

Note, normally we don't do absolute time synchronization i.e. the propagation delay is not calculated. The first channel tap of the channel represents the time of arrival of the first path and that is what the reference for the rest of the channel taps is set as. In modern 5G systems, we have positioning systems, where we require the time of arrival of the first path. In this we only care about aligning the receiver with the first arrival path and the propagation delay will not be calculated in this simulation.

In the receiver since we do the signal processing at the baseband, the passband signal is downconverted at the receiver. The transmitter and receiver clocks may not be at the exact same

frequency due to manufacturing defects, temperature, or Doppler hence the baseband signal has a residual frequency. In OFDM system this can cause ICI and loss of orthogonality between the sub-carriers hence this needs to be removed by frequency offset techniques.

3.3.2 System model and Results

We use two particular OFDM symbols to do frequency and time synchronization. In the first synchronization OFDM symbol s_1 we set the odd sub-carriers to be 0. Let the time domain equivalent of symbol s_1 be denoted as $x[n], n \in (1, N)$. Nulling the odd sub-carriers ensures that for all n within the symbol $x[n] = x[n + N/2]$. Now our metric is a correlator. We pick the first $N/2$ input samples and correlate it with $N/2$ samples at a delay of $N/2$. Mathematically, if $r[n]$ is the input time domain signal at the receiver:

$$P(n) = \sum_{k=0}^{\frac{N}{2}-1} r[n+k] r^*[kn+k+\frac{N}{2}] \quad (7)$$

$$R(n) = \sum_{k=0}^{\frac{N}{2}-1} |r[kn+k+\frac{N}{2}]|^2$$

$$M(n) = \frac{|P(n)|^2}{R(n)^2} \quad (8)$$

Now we collect enough samples in our buffer, say $2N$ time samples and calculate $M(n)$ and plot it as below:

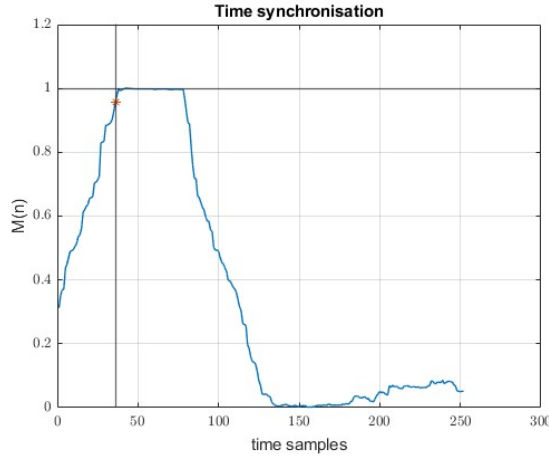


Figure 16: The metric $M(n)$ plotted after introduction of a random delay between 1 and 100 time samples

The timing estimate is simply the first time that $M(n)$ reaches the value 1. $M(n)$ was plotted and the first index at which it reaches 95% of the maximum value is the estimate of the timing offset.

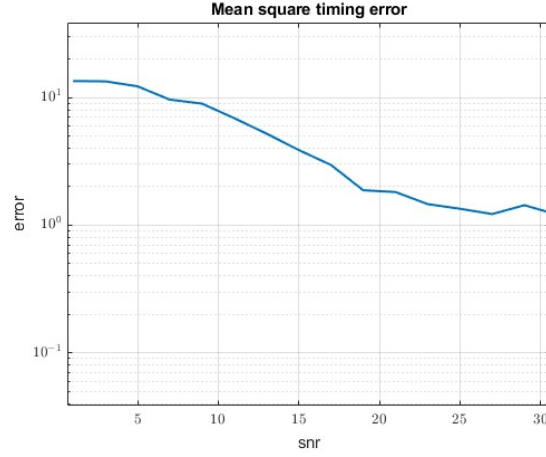


Figure 17: Mean absolute timing error vs SNR

The fractional frequency estimator is simply

$$\hat{f}_o = \frac{\angle(P(n_{opt}))}{\pi} \quad (9)$$

Now after removing the timing offset and fractional offset, we remove the integer frequency offset. For this, we use the second OFDM symbol. We set the second ofdm symbol as $s_2 = g \cdot s_1(1:2:end)$. Here g is a sequence with good Autocorrelation properties. In this simulation, a Golay sequence was used [1]. At the receiver, we convert s_1 and s_2 to the frequency domain. Now the residual integer frequency offset can be visualized as below:

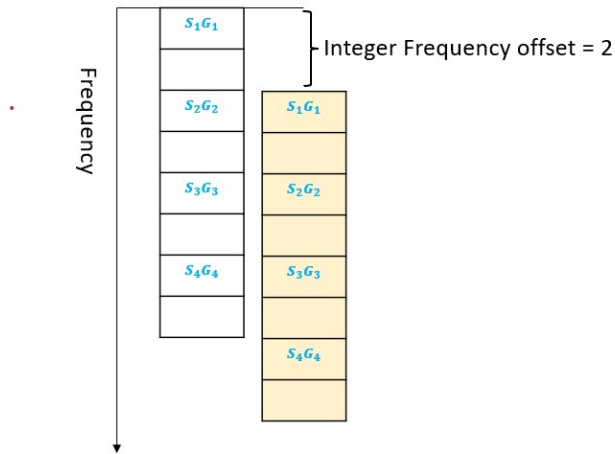


Figure 18: Integer frequency offset

$$\begin{aligned}
\Gamma_1 &= \mathbf{D}_N \bar{\mathbf{r}}_1 \\
&= \mathbf{\Gamma}_{s_1} + \nu_1 \\
\Gamma_2 &= \mathbf{D}_N \bar{\mathbf{r}}_2 \\
&= \mathbf{\Gamma}_{s_2} + \nu_1
\end{aligned} \tag{10}$$

The integer offset can be found by first removing the effect of the channel and also removing the symbols leaving behind the shifted Golay sequence.

$$\mathbf{v} = \text{sgn}(\Re(\Gamma_1(1:2:end) \cdot \Gamma_2(1:2:end)^*)) \tag{11}$$

Now on doing a matched filter with the original Golay sequence, we get a peak at half the value of the integer frequency offset.

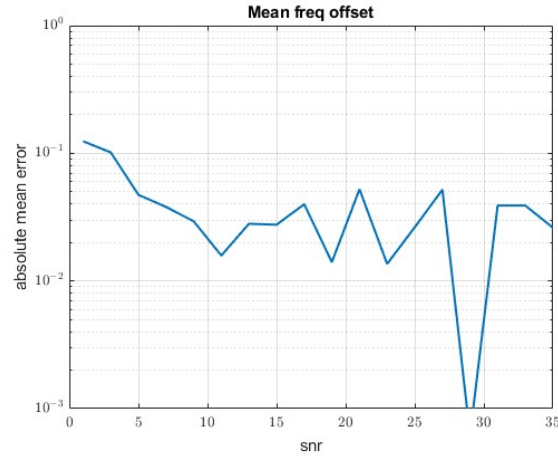


Figure 19: Mean frequency offset error

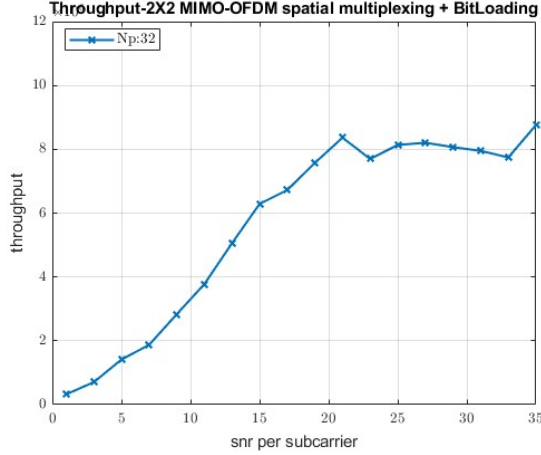


Figure 20: Throughput for a 2×2 Spatially multiplexed MIMO-OFDM system after time and frequency synchronization with channel estimation using 32 pilots

Note: The frequency and throughput plots are jagged and contain the results for just 1 set of pilots since this simulation takes a while to run.

4 Conclusion

- We first create a time-varying, frequency-selective, spatial MIMO channel in the first part with controllable parameters like Doppler spread, Delay spread and Angle dependence for a 2×2 MIMO system.
- We exploit the spatial diversity by using the Alamouti coding scheme to reduce the BER without loss in throughput for MIMO-OFDM.
- We use spatial multiplexing to exploit the spatial diversity by using an MMSE receiver architecture to increase the throughput for MIMO-OFDM.
- Now we do channel estimation for MIMO OFDM and find an optimum number of pilots to optimize throughput empirically
- On top of the previous system, we employed bit-loading to exploit the frequency diversity and further increase the throughput.
- At the end, we covered how to time and frequency synchronize a MIMO OFDM system using two specially designed OFDM symbols. One contains symbols on the even carriers with the odd ones nulled out and the second one contains the same symbols multiplied by an orthogonal sequence like a Golay Code. We first find the timing offset and fractional

frequency offset. After correcting for that we use the Golay sequence on the second OFDM symbol to find the residual integer frequency offset.

References

- [1] Y. Li, “A construction of general qam golay complementary sequences,” *IEEE Transactions on Information Theory*, vol. 56, no. 11, pp. 5765–5771, 2010.